A EUROPEAN JOURNAL

CHEMPHYSCHEM

OF CHEMICAL PHYSICS AND PHYSICAL CHEMISTRY

Accepted Article

Title: Insight into interactions of amyloid beta sheets with graphene flakes: Scrutinizing the role of aromatic residues in amyloids interacting with graphene

Authors: Snežana D. Zarić, Dragana Bozinovski, Predrag Petrovic, and Mililvoj Belic

To be cited as: *ChemPhysChem* 10.1002/cphc.201700847

Link to VoR: http://dx.doi.org/10.1002/cphc.201700847

A Journal of

ChemPubSoc Europe

WILEY-VCH

www.chemphyschem.org

ARTICLE WILEY-VCH

Insight into interactions of amyloid beta sheets with graphene flakes: Scrutinizing the role of aromatic residues in amyloids interacting with graphene

Dragana M. Božinovski,[b] Predrag V. Petrović,[b] Milivoj R. Belić,[b] and Snežana D. Zarić*[a,b]

Abstract: The interaction of amyloid β-sheet segments with graphene flake models is investigated using the density functional theory (DFT). The structure of β-sheets of selected amyloid segments is based on the crystal structures obtained from the Protein Data Bank. Our study, based on the DFT calculations on model systems, indicates that the interaction in amyloid-graphene aggregates can be stronger than the interactions for respective amyloid-amyloid aggregates. The results also indicate an important specific role of aromatic side chains in amyloid-graphene interactions. This work confirms recent experimental evidence that graphene and its modifications inhibit the aggregation of β-amyloid peptides.

Introduction

In the past decade, the use of nanotechnology and carbon nanomaterials has produced a multitude of innovations that have built up new opportunities not only in the modern materials science, but in different areas of medicine, engineering and technology as well.[1–4] A combination of nanotechnology with the study of material properties has opened enormous possibilities for use in different systems, thereby providing plenty of applications of nanomaterials in various biomedical and biological fields like therapeutics, cancer research, drug and gene delivery or bioimaging. Nanoparticles are relatively small in size, up to 100 nm, which makes them comparable to large biomolecules such as proteins, nucleic acids or cell membranes, and allows them to interact on a cellular level. One of the promising characteristics of carbon nanoparticles is the possibility to interact with the misfolding and aggregation of proteins, making these particles potentially a powerful tool to fight different diseases.[5–7] Among those, Alzheimer's disease – a neurodegenerative dementia most likely caused by the production and deposition of β-amyloid peptides in the brain[8–12] – is probably the greatest problem of all and the most promising candidate for potential treatment with nanoparticles. Altogether, the accumulation of a high amount of peptide or protein aggregates can lead to immense problems on cellular level, for example by directly disturbing vital cell functions, exerting toxicity by disrupting intracellular transport or by crushing protein degradation pathways.[10,13,14]

Among the most promising carbon nanoparticles that can help in interrupting protein aggregation are the graphene flakes. Graphene, a carbon sheet-based nanomaterial, represents a planar sheet of sp^2 hybridized carbon atoms, introduced by Geim and Novoselov.[15] During the last few years, graphene and graphene oxide – GO (an oxidized form of graphene) became important in many research studies, due to their extraordinary electronic, mechanical and biostructural characteristics.[16–20] Aggregation of amyloid beta (Aβ) with graphene and GO has been studied experimentally.[21–23] Mahmoudi and colleagues demonstrated that, through adsorption of amyloid monomers, large flakes of GO sheets inhibit the Aβ fibrillization.[23] Yang and colleagues have shown that fibrillization of Aβ monomers can be inhibited by graphene nanosheets and moreover, graphene can cut mature amyloid fibrils into pieces and clear it.[24] Another modification of graphene, the graphene quantum dot (GQD) – a single or a few-layer graphene of a size that is less than 100 nm – was experimentally used for inhibition of Aβ1-42 peptide aggregation, with additional benefit of a reduced cytotoxicity.[25]

Here, we are interested in investigating the interaction of model graphene flakes with the β-sheets of amyloid segments, based on the crystal structures obtained from the Protein Data Bank (PDB).[26] In the past few years a couple of studies were associated with the investigation of interactions between graphene flakes (or graphene "molecules") and amyloid fibrils using classical molecular force field.[27–30] Our research is the first to utilize density functional theory (DFT) to study the interactions between the two molecular systems. We used six different amyloid beta sheet models and graphene flake segments, to calculate energies between these interacting systems.

Methodology Section

All calculations were performed using the Gaussian 09 [rev. D.01] suite of programs.[31] Model systems of amyloids used in these calculations are based on the crystal structures from the PDB. Hydrogen atoms have been added by ArgusLab software (ver. 4.0.1), since their positions were not determined by X-ray crystallography in the PDB structures.[32] All amino acids were neutralized, in order to avoid influence of the charges on the calculations.

[a] Prof. Dr. S. D. Zarić
Department of Chemistry
University of Belgrade
Studentski trg 12-16, 11000 Belgrade, Serbia
E-mail: szaric@chem.bg.ac.rs; snezana.zaric@qatar.tamu.edu
[b] Dr. D. M. Božinovski, Dr. P. V. Petrović, Prof. Dr. M. R. Belić, Prof. Dr. S. D. Zarić
Science Program
Texas A&M University at Qatar
Texas A&M Engineering Building, Education City, Doha, Qatar

Supporting information for this article is given via a link at the end of the document.

A graphene flake molecule was modelled by creating a model system of finite size, consisting of carbon atoms arranged in honeycomb pattern, with hydrogen atoms capping the graphene flake at the outer ring (Figure S1, SI). Different size models of graphene flakes were considered, with molecular formulas $C_{216}H_{36}$, $C_{294}H_{42}$, $C_{384}H_{48}$, and $C_{486}H_{54}$ (Figure S1, SI). For the graphene, all atoms were optimized to find the most stable structure, using the B3LYP-D3/6-31G* method.[33–38] In the calculations on peptides, only positions of hydrogen atoms were optimized, because of the possible steric hindrance (bad contacts) that can be caused by hydrogens that have not been optimally positioned by ArgusLab; the rest of the atoms were kept rigid, as they are in the crystal structures of amyloids. Because of the size of the system, in our calculations we did not include influence of environment.

The interaction energies were calculated at the B3LYP-D3/6-31G* level of theory with the BSSE correction,[39] which is computationally tractable for large amyloid segments.

For the contact of side-chains with the graphene we applied criteria that the normal distance between the C (N) atom and the graphene is less than 4.5 Å, while for the nonaromatic side chains, an additional criterion that the angle between C-H (N-H) bond and the graphene plane is between 30° and 90°.

Results and Discussion

In this work, we have analyzed interactions of β-sheets of amyloid segments with a model of graphene flake molecule. For β-sheets, we used amyloid segments isolated from the Aβ1-42 peptide with the PDB entry codes 2Y29 (16-KLVFFA-21 Form III), 2Y2A (16-KLVFFA-21 Form I), 3OW9 (16-KLVFFA-21 Form II), 2Y3J (30-AIIGLM-35), 2Y3L (35-MVGGVVIA-42 Form II) and 3Q2X (27-NKGAII-32),[40] as deposited in the PDB. These particular amyloid segments were chosen so as to utilize our recent results on the interaction energies between amyloid β-sheets, where the same segments were used.[41] Data obtained in the previous study provided a good foundation for comparing the interaction energies for amyloid aggregates on the one side, with the amyloid-graphene aggregates on the other side. Model systems used in the calculations of interaction energies were constructed using one tetramer β-sheet of selected amyloids and the graphene flake (Figures 1, 2 and 3).

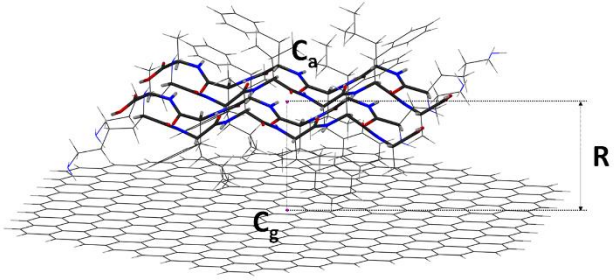

Figure 1. Model system presenting interaction of 2Y29 β-sheet tetramer and graphene $C_{384}H_{48}$ flake. C_a, center of mass of the amyloid β-sheet; C_g, center of mass of the graphene flake; R, normal distance between the graphene sheet and the mean plane of amyloid backbone atoms.

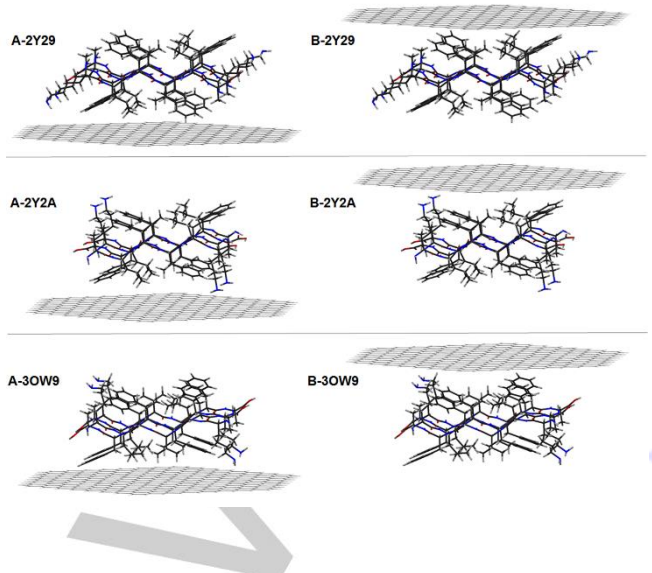

Figure 2. Aggregates of β-sheets of amyloid structures containing aromatic amino acids, 2Y29, 2Y2A, and 3OW9, with the graphene $C_{384}H_{48}$ flake. Left column: the bottom (A) side of the amyloids interacts with the graphene flake; right column: the top (B) side of the amyloids interacts with the graphene flake.

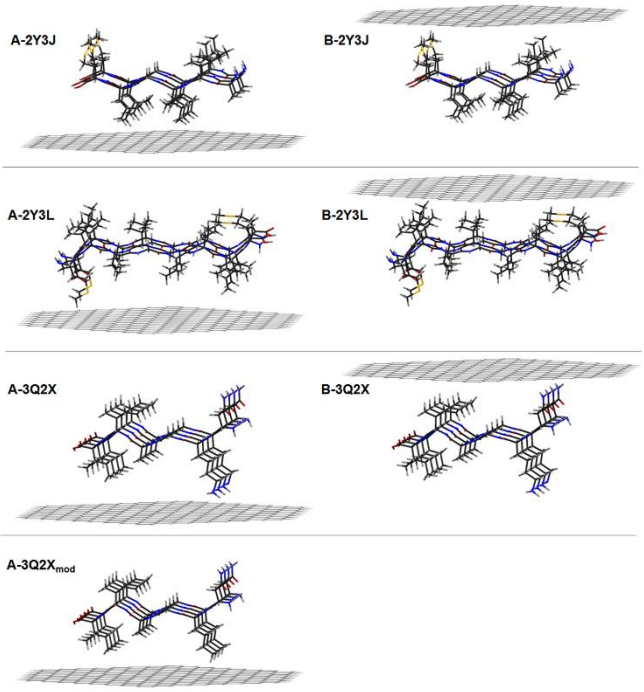

Figure 3. Aggregates of β-sheets of amyloid structures not containing aromatic amino acids, 2Y3L, 2Y3J, and 3Q2X/3Q2X_{mod}, with the graphene $C_{384}H_{48}$ flake. Left column: the bottom (A) side of the amyloid interacts with the graphene flake; right column: the top (B) side of the amyloid interacts with the graphene flake. The structure for the B side of 3Q2X_{mod} is identical to the structure for the B side of 3Q2X, and thus it is omitted.

Table 1. Interaction energies calculated using B3LYP-D3/6-31G* method (in kcalmol^{-1}) for the interaction between two tetramer β-sheets of amyloid structures,[41] and between the tetramer β-sheet and graphene $C_{384}H_{48}$ flake (Figures 2 and 3).

	Structure	Interaction between β-sheets[a]	Interaction between β-sheet and $C_{384}H_{48}$	R[b] (Å)
Aromatic amyloids	A-2Y29[c]	-40.18	-62.39	7.5
	B-2Y29		-61.95	7.5
	A-2Y2A	-40.04	-38.56	8.6
	B-2Y2A		-37.79	8.6
	A-3OW9	-52.92	-63.22	7.7
	B-3OW9		-46.35	8.2
Nonaromatic amyloids	A-2Y3J	-51.53	-43.17	7.9
	B-2Y3J		-33.72	8.6
	A-2Y3L	-42.62	-22.15	9.2
	B-2Y3L		-61.42	7.3
	A-3Q2X	-125.58	-26.48	9.2
	B-3Q2X		-37.14	8.7
	A-3Q2X$_{mod}$[d]	-75.12	-36.73	8.1

[a] data from the reference 41; [b] distance R between amyloid β-sheet and graphene flake (as shown in Figure 1); [c] A and B designate the sides of the amyloid (Figures 2 and 3, Figure S2 SI) involved in the interaction with the graphene flake; [d] a model system modified to remove the influence of hydrogen bonds, as explained in SI and reference 41.

Several sizes of the graphene flake were considered (Figure S1, SI), since the model system had to be small enough to be computationally practical, yet large enough to avoid interaction with the hydrogen atoms at the graphene flake edge. It was found that the graphene flake with the molecular formula $C_{384}H_{48}$ is the most suitable for our study, since interaction energy of this graphene model did not change significantly compared to the large graphene model $C_{486}H_{54}$ (Table S1, SI). The planes of the β-sheet and graphene flake were kept parallel relative to each other, while the centroids of the amyloid backbone atoms and the graphene flake were aligned with each other (Figure 1). Since each amyloid β-sheet has two sides, the bottom (A) and the top (B) (Figures 2 and 3, Figure S2 SI), energies were calculated for the interaction of both amyloid sides with the graphene flake.

The normal distance R – the distance between the mean plane of the amyloid β-sheet and the plane of the graphene flake (Figure 1) – was varied in increments of 0.1 Å, and the interaction energies were calculated for each value of R. The energies of the strongest interactions and the corresponding distances R for each of the studied systems are reported in Table 1. More details on the model system construction can be found in SI.

The data in Table 1 and in Figure 4 show that the normal distance R is in correlation with the interaction energy between an amyloid and the graphene flake. On average, the distances are shorter for the amyloids with aromatic amino acids. Moreover, comparing structures with similar distances, one can notice that the amyloids with aromatic residues have stronger interactions than the amyloids without aromatic amino acids, indicating a stronger interaction of an aromatic ring with the graphene.

The type of interaction and the number of contacts between the amyloid side-chains and the graphene flake depend on the amyloid structure (Figures 2 and 3). To recognize contact of side-chains with the graphene, we applied criteria that were described in Methodology Section. In all model systems, there are CH/π and NH/π interactions with graphene, while in the model systems with aromatic amino acids, there are also interactions of the aromatic rings with graphene. The data on the model systems show that the aromatic rings form interactions where the angle between the ring and the plane of the graphene

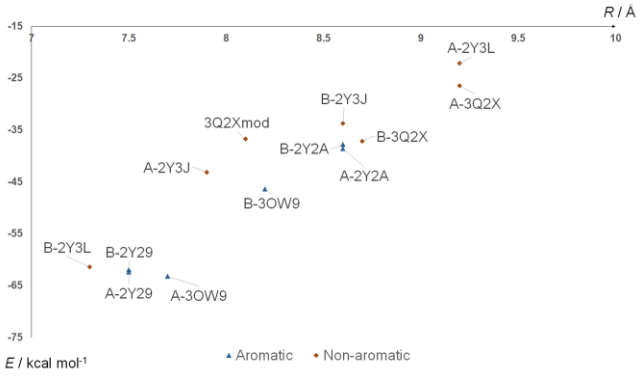

Figure 4. The distance *vs* interaction energy graph for the interaction of amyloid β-sheets with the graphene $C_{384}H_{48}$ flake.

has values between 20° and 40°.[42-44] The number of contacts between the side-chains of amyloids and the graphene flake is corelated with the strength of interactions; the graph in Figure 5 indicates that more contacts result in stronger interactions, and *vice versa*. Data in Figure 5 show that the amyloids with aromatic amino acids have stronger interactions than amyloids

without aromatic amino acids, even in the case when the number of contacts is the same. This indicates that the interaction of an aromatic ring with the graphene flake,

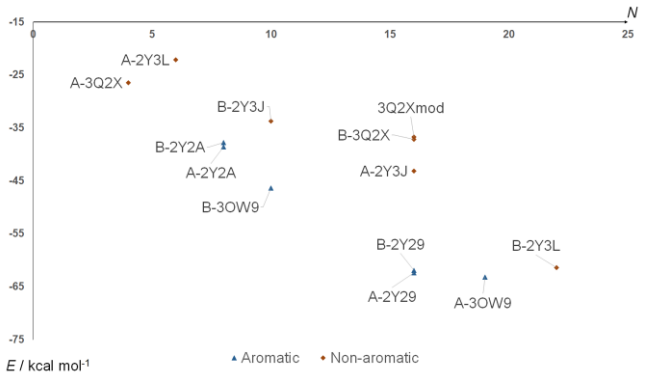

Figure 5. The number of contacts *vs* interaction energy graph for the interaction of amyloid β-sheets with the graphene $C_{384}H_{48}$ flake.

considered as one contact, is probably stronger than the CH/π and NH/π interactions. The similar conclusion that aromatic amino acids form stronger interactions was made above, based on the normal distances R (Figure 4). As one can anticipate, in the systems with smaller distance R, number of contacts is larger and vice versa as data in Figure 6 indicate. Again, one can notice difference for amyloids with and without aromatic residues; for the similar number of contacts, amyloids with aromatic have shorter distance R, additionally indicating stronger interactions of aromatic residues.

The data in Table 1 show that the interaction energies between the amyloid β-sheet and the graphene flake fall within a broad range, varying from -22.1 kcalmol^{-1} to -63.2 kcalmol^{-1}. With a few exceptions, the interactions for the amyloids with aromatic amino acids, 2Y29, 2Y2A, and 3OW9, are stronger than the energies for the amyloids without aromatic amino acids, 2Y3L, 2Y3J, and 3Q2X. Also, the amyloids with aromatic amino acids have amyloid-graphene interactions that are, with one exception, stronger (or at least similar in strength) than the amyloid-amyloid interactions. On the other hand, for the amyloids without aromatic amino acids, the amyloid-graphene interactions are, with one exception, much weaker than the amyloid-amyloid interactions. These data, together with data in Figures 4, 5 and 6, again indicate stronger interactions of aromatic amino acids with graphene flake.

The number of contacts and the distances R are similar for the A and B sides for some of the amyloids (2Y29, 2Y2A), while for other amyloids they are very different (Figures 4 and 5, Table 1).

The number of contacts depends on the side chains that are on a particular side of the β-sheet, as well as on the conformation of the side chains. The three amyloids with aromatic amino acids, 2Y29, 2Y2A, 3OW9, and amyloid 2Y3L without aromatic amino acids, have antiparallel orientations of the polypeptide strands in the β-sheet, hence they have the same side chains on both sides of the β-sheet, A and B, so the difference between A and B side interactions depends only on the conformation of the chains. Amyloids 2Y3J, 3Q2X, and $3Q2X_{mod}$, without aromatic amino acids, have parallel orientation, hence, they have different amino acids on the A and B sides that form interactions with the graphene flake.

The three amyloids with aromatic amino acids have the same sequence (KLVFFA) and antiparallel orientations of polypeptide strands, however, different conformations of the side-chains lead to different amyloid-graphene interaction energies (Figures 4 and 5, Table 1). For two amyloid structures, 2Y29 and 2Y2A, the amyloid-graphene interaction energies for A and B sides are similar, and also the distances R and the number of contacts for A and B sides are the same. One of those, 2Y29 has quite strong, above 60 kcalmol^{-1} for both A and B sides. These interactions are 15 to 40 kcalmol^{-1} stronger than the amyloid-graphene interactions for other structures (except for A-3OW9 and B-2Y3L) and more than 20 kcalmol^{-1} stronger than the amyloid-amyloid interaction for the same, 2Y29, structure (Table 1). Strong interactions correlate with short distances R (7.5 Å) and relatively large number of contacts between the amyloid and graphene (Figures 4 and 5). Among these contacts, there are four of the aromatic/graphene type.

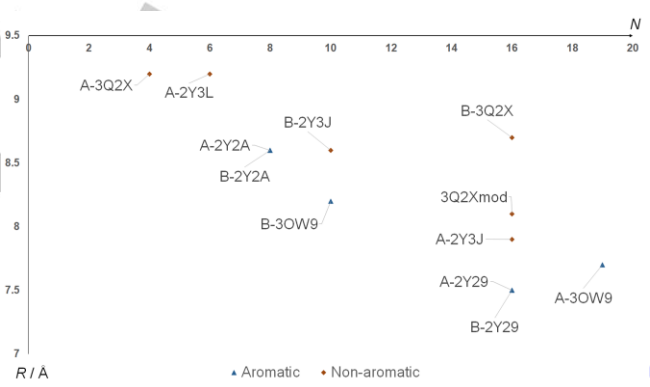

Figure 6. The distance *vs* number of contacts for the interaction of amyloid β-sheets with the graphene $C_{384}H_{48}$ flake.

The other amyloid structure with similar interaction energies for A and B sides, 2Y2A, exhibits significantly weaker amyloid-graphene interactions, about 38 kcalmol^{-1}; these interactions are the weakest among the interactions of amyloids with aromatic amino acids. These amyloid-graphene interactions are ofrelatively long distances R (Table 1 and Figure 4) and display a small number of contacts (Figure 5), with only two contacts of the aromatic side chains with the graphene.

The third amyloid structure with aromatic amino acids, 3OW9, has very different interaction energies for A and B sides (Table 1), in spite of the antiparallel orientations of polypeptide strands and the same side chains on both A and B sides of the β-sheet. Hence, the difference in energies is caused by different conformations of the side chains. The A-3OW9/$C_{384}H_{48}$ model system exhibits the strongest interaction (-63.2 kcalmol^{-1}) among all the amyloid-graphene aggregates. For the B-3OW9/$C_{384}H_{48}$ model system, the interaction is significantly weaker, it amounts to -46.35 kcalmol^{-1}. The interaction for the A side is around 10 kcalmol^{-1} stronger than the amyloid-amyloid interaction , while

for the B side it is around 7 kcalmol^{-1} weaker (Table 1). Two sides display different number of contacts with the graphene (Figure 5), and the number of aromatic ring involved in the interactions of side A is twice (four) that of side B has (two).

For amyloids without aromatic amino acids, amyloid-graphene interactions are, with a few exceptions, weaker than the interactions between amyloids with aromatic amino acids and graphene (Table 1), as mentioned above. All interactions, except one, are weaker than the corresponding interactions between two amyloid β-sheets.

For two amyloids without aromatic amino acids (2Y3J, and 3Q2X), the polypeptide strands are parallel and the sides A and B differ in the number of amino acids involved in the interaction with the graphene flake, as well as in normal distances R, so different interaction energies, are obtained for A and B sides (Table 1). Amyloid 2Y3L has antiparallel orientation of strands, hence the same side chains on both A and B sides, however, interaction energies are very different for different sides, because of the large difference in the side chain conformations (Figure 3). The A-2Y3L/$C_{384}H_{48}$ model system displays the weakest interaction (-22.15 kcalmol^{-1}) among all the amyloid-graphene aggregates, which is about 20 kcalmol^{-1} weaker than the corresponding amyloid-amyloid interaction. However, the B-2Y3L/$C_{384}H_{48}$ model system exhibits quite strong interaction, -61.42 kcalmol^{-1}, one of the strongest among the studied systems (Table 1), and about 20 kcalmol^{-1} stronger than the respective amyloid-amyloid interaction energy (Table 1).

The model systems made from 3Q2X structure show the most significant difference between the amyloid-graphene interaction energy and the amyloid-amyloid interaction energy (Table 1); the amyloid-graphene interactions are 40 - 100 kcalmol^{-1} weaker than the amyloid-amyloid interactions. Due to not particularly favorable interactions of the amyloid side-chains with the graphene flake, the distances between the two sheets are relatively large; the A-3Q2X/$C_{384}H_{48}$ model system possesses the largest distance, the smallest number of interactions and the weakest interaction (Figures 4 and 5, Table 1).

The next step in this research would be to optimize model systems, to calculated interactions energies of optimized systems, and to to see if the same conclusions apply.

As previously mentioned, it was experimentally established that the amyloid peptides, and particularly Aβ, form aggregates with graphene sheets, graphene-oxide, or graphene quantum dots.[21–25] Yang and colleagues have demonstrated through molecular dynamics simulations that the peptides and graphene form strong dispersion interactions, enhanced by the π-π stacking between graphene sheets and the aromatic residues of β-amyloid.[24] Our study reveals similar behavior but from a different point of view. The data we obtained show that the amyloid structures with aromatic side chains typically form interactions with graphene flake that are stronger, or similar in strength, compared to their respective β–sheet interactions. However, the presence of aromatic amino acids in the sequence of amyloids could not be considered as the decisive factor that influences the interaction energies by itself. A favorable conformation of the side-chains, leading to a larger number of contacts between the amyloids and graphene seems to exert even more decisive impact. In addition, the correlation of interaction energies with the number of interactions, and with the distance R between the amyloid β–sheet and the graphene flake, indicate stronger interaction of aromatic rings with the graphene.

Conclusions

As the material with exceedingly wide range of interesting properties (physical, optical, structural, biological), graphene has been the subject of intense interest and numerous studies across different fields. Its ability to form aggregates with different organic molecules was elucidated both experimentally and theoretically. Here, this is accomplished by the use of DFT calculations. Specific interactions with the Aβ protein segments were shown to inhibit the formation of amyloid fibril plaques, a process strongly suspected as being responsible for several debilitating neurodegenerative diseases.

Our calculations on model systems of amyloid-graphene aggregates have shown that the amyloid β–sheets display strong interactions with graphene. Interactions of graphene with amyloids that possess aromatic amino acids in the sequence are stronger than the interactions with amyloids without aromatic amino acids. Most importantly, our calculations indicate stronger interaction of graphene with amyloids, as compared to the mutual interaction of amyloid β–sheets. They also imply an important specific role of the aromatic rings in the amyloid-graphene interactions. This is in accordance with the experimental observations that graphene and its modifications (GO, GQD) interact strongly with the aromatic amino acids in amyloid side-chains, and inhibit the aggregation of amyloid β fibrils.

Acknowledgements

This publication was made possible by the NPRP awards [NPRP7-665-1-125 and NPRP8-425-1-087] from the Qatar National Research Fund (a member of The Qatar Foundation). The statements made herein are solely the responsibility of the authors.

Keywords: Density functional calculations • Graphene • Amyloid beta-peptides • Noncovalent interactions • PDB

[1] D. Docter, S. Strieth, D. Westmeier, O. Hayden, M. Gao, S. K. Knauer and R. H. Stauber, *Nanomedicine* **2015**, *10*, 503–519.
[2] P. N. Navya and H. K. Daima, *Nano Converg.* **2016**, *3*, 1-14.
[3] Ž. Krpetić, S. Anguissola, D. Garry, P. M. Kelly and K. A. Dawson, *Adv. Exp. Med. Biol.* **2014**, *811*, 135–156.
[4] K. Cai, A. Z. Wang, L. Yin and J. Cheng, *J. Control. Release* **2017**, S0168-3659(16)30527-2.
[5] C. Cabaleiro-Lago, F. Quinian-Pluck, I. Lynch, S. Lindman, A. M. Minogue, E. Thulin, D. M. Walsh, K. A. Dawson and S. Linse, *J. Am. Chem. Soc.* **2008**, *130*, 15437–15443.
[6] M. Chin-Chan, J. Navarro-Yepes and B. Quintanilla-Vega, *Front. Cell. Neurosci*. **2015**, *9*, 124, 1-22.

[7] D. K. Ban and S. Paul, *ACS Appl. Mater. Interfaces* **2016**, *8*, 31587–31601.
[8] C. M. Dobson, *Cold Spring Harb. Perspect. Biol.* **2017**, *9(6)*, a023648.
[9] P. Nguyen and P. Derreumaux, *Acc. Chem. Res*. **2014**, *47*, 603–611.
[10] S. C. Meredith, *Ann. N. Y. Acad. Sci.*, **2005**, *1066*, 181–221.
[11] R. Tycko and R. B. Wickner, *Acc. Chem. Res*. **2013**, *46*, 1487–1496.
[12] N. Carulla, M. Zhou, E. Giralt, C. V. Robinson and C. M. Dobson, *Acc. Chem. Res.* **2010**, *43*, 1072–1079.
[13] J.-C. Lin and H.-L. Liu, *Curr. Drug Discov. Technol.* **2006**, *3*, 145–53.
[14] X. Fernàndez-Busquets, N. S. de Groot, D. Fernandez and S. Ventura, *Curr. Med. Chem.* **2008**, *15*, 1336–49.
[15] K. S. Novoselov, A. K. Geim, S. V. Morozov, D. Jiang, Y. Zhang, S. V. Dubonos, I. V. Grigorieva and A. A. Firsov, *Science* **2004**, *306*, 666–669.
[16] D. Chen, L. Tang and J. Li, *Chem. Soc. Rev.* **2010,** *39*, 3157-3180.
[17] D. R. Dreyer, S. Park, C. W. Bielawski and R. S. Ruoff, *Chem. Soc. Rev.* **2010**, *39*, 228–240.
[18] O. C. Compton, S. T. Nguyen, *Small* **2010**, *6*, 711–723.
[19] Y. Zhu, S. Murali, W. Cai, X. Li, J. W.Suk, J. R. Potts, R. S. Ruoff, *Adv. Mater.* **2010**, *22*, 3906–3924.
[20] S. Ullah, P. A. Denis, F. Sato, *ChemPhysChem* **2017**, *18*, 1864 –1873.
[21] M. Li, X. Yang, J. Ren, K. Qu and X. Qu, *Adv. Mater.* **2012**, *24*, 1722–1728.
[22] C. Li, J. Adamcik and R. Mezzenga, *Nat. Nanotechnol.* **2012**, *7*, 421–427.
[23] M. Mahmoudi, O. Akhavan, M. Ghavami, F. Rezaee and S. M. A. Ghiasi, *Nanoscale* **2012**, *4*, 7322–7325.
[24] Z. Yang, C. Ge, J. Liu, Y. Chong, Z. Gu, C. A. Jimenez-Cruz, Z. Chai and R. Zhou, *Nanoscale*, 2015, **7**, 18725–18737.
[25] Y. Liu, L.-P. Xu, W. Dai, H. Dong, Y. Wen and X. Zhang, *Nanoscale* **2015**, *7*, 19060–19065.
[26] H. M. Berman, J. Westbrook, Z. Feng, G. Gilliland, T. N. Bhat, H. Weissig, I. N. Shindyalov and P. E. Bourne, *Nucleic Acids Res.* **2000**, *28*, 235–242.
[27] G. Qing, S. Zhao, Y. Xiong, Z. Lv, F. Jiang, Y. Liu, H. Chen, M. Zhang and T. Sun, *J. Am. Chem. Soc.* **2014**, *136*, 10736–10742.
[28] L. Baweja, K. Balamurugan, V. Subramanian and A. Dhawan, *J. Mol. Graph. Model.* **2015**, *61*, 175–185.
[29] Wang, X. J. K. Weber, L. Liu, M. Dong, R. Zhou and J. Li, *Nanoscale* **2015**, *7*, 15341–15348.
[30] E. S. Kryachko, in *Applications of Density Functional Theory to Biological and Bioinorganic Chemistry*, (Eds.: M. V. Putz, M. D. P. Mingos), Springer-Verlag, Berlin Heidelberg, **2013**, *150*, pp. 65-96.
[31] M. J. Frisch, G. W. Trucks, H. B. Schlegel, G. E. Scuseria, M.A. Robb, J. R. Cheeseman, G. Scalmani, V. Barone, B. Mennucci, G. A. Petersson, H. Nakatsuji, M. Caricato, X. Li, H. P. Hratchian, A. F. Izmaylov, J. Bloino, G. Zheng, J. L. Sonnenberg, M. Hada, M. Ehara, K. Toyota, R. Fukuda, J. Hasegawa, M. Ishida, T. Nakajima, Y. Honda, O. Kitao, H. Nakai, T. Vreven, J. A. Jr Montgomery, J. E. Peralta, F. Ogliaro, M. Bearpark, J. J. Heyd, E. Brothers, K. N. Kudin, V. N. Staroverov, R. Kobayashi, J. Normand, K. Raghavachari, A. Rendell, J. C. Burant, S. S. Iyengar, J. Tomasi, M. Cossi, N. Rega, N. J. Millam, M. Klene, J. E. Knox, J. B. Cross, V. Bakken, C. Adamo, J. Jaramillo, R. Gomperts, R. E. Stratmann, O. Yazyev, A. J. Austin, R. Cammi, C. Pomelli, J. W. Ochterski, R. L. Martin, K. Morokuma, V. G. Zakrzewski, G. A. Voth, P. Salvador, J. J. Dannenberg, S. Dapprich, A. D. Daniels, Ö. Farkas, J. B. Foresman, J. V. Ortiz, J. Cioslowski, and D. J. Fox, Gaussian, Inc., Wallingford CT, **2009**.
[32] M. A. Thompson, *ACS meeting*, Philadelphia, **2004**, *172*, CINF 42, PA.
[33] A. D. Becke, *J. Chem. Phys.* **1993**, *98*, 5648-5652.
[34] C. Lee, W. Yang, R. G. Parr, *Phys. Rev. B* **1988**, *37*, 785-789.
[35] S. Grimme, *WIREs Comput. Mol. Sci.* **2011**, *1*, 211-228.
[36] S. Grimme, J. Antony, S. Ehrlich, H. Krieg, *J. Chem. Phys.* **2010**, *132*, 154104-154119.
[37] G. A. Petersson, A. Bennett, T. G. Tensfeldt, M. A. Al-Laham, W. A. Shirley, J. Mantzaris, *J. Chem. Phys.* **1988**, *89*, 2193-2218.
[38] G. A. Petersson, M. A. Al-Laham, *J. Chem. Phys.* **1991**, *94*, 6081-6090.
[39] S. F. Boys, F. Bernardi, *Mol. Phys.* **1970**, *19*, 553−566.
[40] J.-P. Colletier, A. Laganowsky, M. Landau, M. Zhao, L. Goldschmidt, D. Flot, D. Cascio, M. R. Sawaya, A. B. Soriaga, D. Eisenberg, *Proc. Natl. Acad. Sci. USA* **2011**, *108*, 16938–16943.
[41] D. B. Ninković, D. P. Malenov, P. V. Petrović, E. N. Brothers, S. Niu, M. B. Hall, M. R. Belić and S. D. Zarić, *Chem. Eur. J.* **2017**, accepted.
[42] D. B. Ninkovic, J. M. Andric, S. N. Malkov, S. D. Zaric, *Phys. Chem. Chem. Phys.* **2014**, *16*, 11173-11177.
[43] D. B. Ninkovic, G. V. Janjic, D. Z. Veljkovic, D. N. Sredojevic, S. D. Zaric, *ChemPhysChem* **2011**, *12*, 3511–3514.
[44] E. C. Lee, D. Kim, P. Jurečka, P. Tarakeshwar, P. Hobza, K. S. Kim, *J. Phys. Chem. A* **2007**, *111 (18)*, 3446–3457.

10.1002/cphc.201700847

ARTICLE

β-amyloid peptide accumulation in the brain is most likely cause of the Alzheimer's disease. Aggregates of β-sheets of amyloid structures with the graphene flake (see picture) were studied by DFT calculations. Graphene flake interactions with amyloid sheets are stronger than interaction of the two amyloid sheets, which confirms experimental observations that graphene inhibits amyloid aggregation.

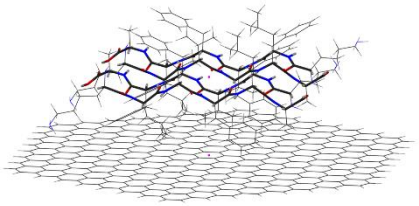

*D. M. Božinovski, P. V. Petrović, M. R. Belić, S. D. Zarić**

Page No. – Page No.

Insight into interactions of amyloid beta sheets with graphene flakes: Scrutinizing the role of aromatic residues in amyloids interacting with graphene